(i) P4501B1: 5′-TCCTGGACAAGTTCTTGAGG-3′ (508 bp) and 5′-TCAAAGTTCTCCGGGTTAGG-3′. (ii) AKR1C1: 5′-CAGGATTGGCCAAGTCCATC-3′ (256 bp) and 5′-CAAAGGACTGGGTCCTCCAA-3′. (iii) NQO1: 5′-CTGATCGTACTGGCTCACTC-3′ (202 bp) and 5′-GAACAGACTCGGCAGGATAC-3′. (iv) GSTM1: 5′-TCACAAGATCACCCAGAGCA-3′ (364 bp) and 5′-AAAGCGGGAGATGAAGTCCT-3′.

P4501A1 (433 bp), 1A2 (309 bp), and glyceraldehyde-3-phosphate dehydrogenase (GAPDH) (546 bp) primers were used from Takara's Human Cytochrome P450 Competitive RT-PCR Set. Quantification of cDNA was performed using a Smart Cycler System (Cepheid, United States), and staining was carried out with SYBR Green I. A 2 $\mu$L portion of the reverse transcriptase mixture was added to a PCR mixture containing 0.2 $\mu$M of each primer, 0.3 mM dNTPs, and 0.05 U Ex Taq DNA polymerase in a final volume of 25 $\mu$L according to Takara Ex Taq R-PCR Version 2.1 for P4501B1 gene and Version 1.0 for other genes with slight modifications. The PCR reactions were performed with Ex Taq polymerase under the following conditions (95 °C for 3 s and 65 °C for 30 s for the GAPDH and P4501A1, 1A2, and 1B1 genes; 95 °C for 3 s and 66 °C for 30 s for the AKR1C1 gene; 95 °C for 3 s and 60 °C for 30 s for the NQO1 gene; and 95 °C for 3 s and 64 °C for 30 s for the GSTM1 gene). PCR amplifications were carried out for 35 cycles for the GAPDH, P4501A1, AKR1C1, NQO1, and GSTM1 genes, for 40 cycles for the P4501A2 gene, and for 45 cycles for the P4501B1 gene. Specificity of the PCR product was determined by melting curve analysis. The expression was then normalized against the expression of GAPDH.

The concentrations producing P4501A1 mRNA equal to 25% of the maximal amount to TCDD were calculated and expressed as $EC_{TCDD25}$. The ratios of the $EC_{TCDD25}$ of B[*a*]P to the $EC_{TCDD25}$ of each of the tested compounds were calculated and were referred to as induction equivalency factors (IEFs).

## Results

**Induction of mRNA of Metabolic Enzymes Measured after Exposure of 5 $\mu$M PAHs and Oxy-PAHs for 24 h.** The amount of P450s (P4501A1, 1A2, and 1B1), AKR1C1, NQO1, and GSTM1 mRNA in HepG2 cells induced by 5 $\mu$M of 20 representative PAHs and oxy-PAHs for 24 h was examined (Figures 2 and 3). The ratio of P4501A1 mRNA levels to GAPDH mRNA of $Me_2SO$ control level was $1.1 \times 10^{-2}$. P4501A1 mRNA was induced by 5 $\mu$M in the case of most PAHs and some oxy-PAHs. B[*a*]P was 40-fold higher than the $Me_2SO$ control (Figure 2A). The five-ring PAHs such as B[*k*]FA, DB[*a,h*]A, and 3-MC and the six-ring IdP were as high as or higher than the levels of induction by B[*a*]P (38- to ~58-fold). The six-ring PAH N[*a*]P induced at the highest level (80-fold) among compounds examined in this study and the four-ring PAHs B[*a*]A and Chr were slightly lower than the levels of induction by B[*a*]P (both were 29-fold). The levels of induction by four-ring oxy-PAHs, NCQ, BAQ, and B[*b*]FO and four-ring PAH and B[*b*]F were also high (21-, 17-, 15-, and 14-fold, respectively), but polycyclic aromatic ketones such as B[*a*]FO and B[*c*]FO showed low induction levels and six-ring PAH, B[*ghi*]Pe, and a representative AhR ligand, $\beta$-NF, which was used for comparison—$\beta$-NF is not an atmospheric pollutant—also showed low activities (3-, 2-, 3-, and 3-fold, respectively). The four-ring PAH, TPh, and five-ring PAK, CPPO, induced P4501A1 mRNA at the same levels as the $Me_2SO$ control. The P4501A1 mRNA induction activity by five-ring PAK, BPO, was under half that of the control values (0.4-fold). The ratio of P4501A2 mRNA levels to GAPDH mRNA of $Me_2SO$ control level was $8.5 \times 10^{-4}$. The tendency was observed that P4501A2 mRNA induction for test chemicals was similar to that of P4501A1 (Figure 2B). The levels of induction by B[*a*]P, B[*a*]A, Chr, B[*b*]FA, B[*k*]FA, DB[*a,h*]A, IdP, N[*a*]P, BAQ, NCQ, and

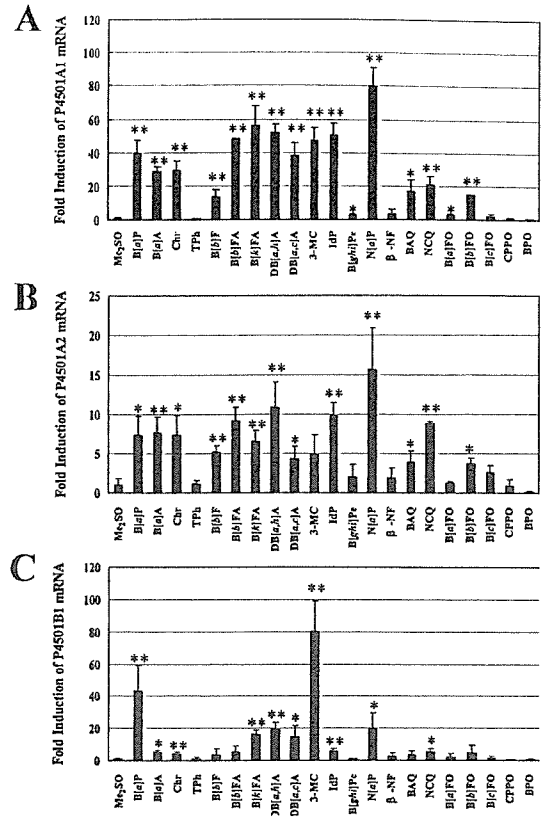


**Figure 2.** Induction of P450s mRNA measured by RT-PCR in HepG2 cells exposed to 5 $\mu$M PAHs and oxy-PAHs for 24 h. (A) P4501A1 mRNA, (B) P4501A2 mRNA, and (C) P4501B1 mRNA were measured. Two asterisks (**) indicate a highly significant difference from control ($p < 0.01$), and one asterisk (*) indicates a significant difference from control ($p < 0.05$) as determined by a *t*-test.

B[*b*]FO were 7-, 8-, 7-, 9-, 7-, 11-, 10-, 16-, 4-, 9-, and 4-fold, respectively. B[*c*]FO, B[*ghi*]Pe, and $\beta$-NF showed low activities (3-, 2-, and 2-fold, respectively). TPh, B[*a*]FO, and CPPO induced P4501A2 mRNA at the same levels as the $Me_2SO$ control. The ratio of P4501B1 mRNA levels to GAPDH mRNA of $Me_2SO$ control level was $3.5 \times 10^{-6}$. In P4501B1 mRNA induction, 3-MC was very high (80-fold) and B[*a*]P was 44-fold followed by N[*a*]P, DB[*a,h*]A, B[*k*]FA, and DB[*a,c*]A (20-, 20-, 16-, and 15-fold, respectively) (Figure 2C). B[*a*]A, Chr, B[*b*]F, B[*b*]FA, IdP, BAQ, NCQ, and B[*b*]FO were 5-, 4-, 4-, 5-, 6-, 4-, 5-, and 5-fold, respectively. The tendency was also observed that both P4501A2 and P4501B1 mRNA induced by BPO were under half that of the control values (0.1- and 0.5-fold, respectively) similar to P4501A1. The mRNA induction levels for each P450 (P4501A1, 1A2, and 1B1) by most AhR active nonoxy-PAHs were higher than AhR active oxy-PAHs at 5 $\mu$M. It was first found that 5 $\mu$M nonoxy-PAHs such as B[*b*]F, DB[*a,c*]A, and N[*a*]P and oxy-PAHs such as BAQ, NCQ, and B[*b*]FO induced CYPs.

The ratio of AKR1C1 mRNA levels to GAPDH mRNA of $Me_2SO$ control level was $3.3 \times 10^{-2}$. AKR1C1 mRNA levels were very high in one oxy-PAH, B[*a*]FO (11-fold to $Me_2SO$ control), and the levels are close to a representative AhR ligand and AP-1 active compound, $\beta$-NF (13-fold to $Me_2SO$ control) (Figure 3A). B[*a*]P, B[*k*]FA, DB[*a,h*]A, NCQ, B[b]FO, and CPPO also induced AKR1C1 mRNA significantly (7-, 7-, 5-, 6-, 5-, and 5-fold, respectively).

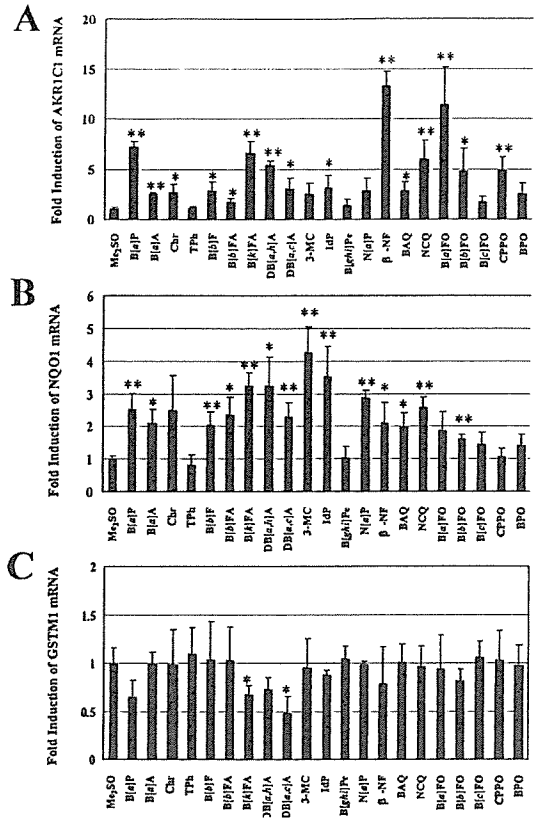


**Figure 3.** Induction for mRNA of metabolic enzymes measured by RT-PCR in HepG2 cells exposed to 5 $\mu$M PAHs and oxy-PAHs for 24 h. (A) AKR1C1 mRNA, (B) NQO1 mRNA, and (C) GSTM1 mRNA were measured. Two asterisks (**) indicate a highly significant difference from control ($p < 0.01$), and one asterisk (*) indicates a significant difference from control ($p < 0.05$) as determined by a *t*-test.

The ratio of NQO1 mRNA levels to GAPDH mRNA of $Me_2SO$ control level was $2.4 \times 10^{-1}$. NQO1 mRNA levels were high for 3-MC and IdP (both were 4-fold to control), and B[*a*]P, Chr, B[*k*]FA, DB[*a,h*]A, N[*a*]P, and NCQ all were 3-fold (Figure 3B). The ratio of GSTM1 mRNA levels to GAPDH mRNA of $Me_2SO$ control level was $8.4 \times 10^{-2}$. No test chemical induced GSTM1 mRNA significantly. However, GSTM1 mRNA levels of B[*a*]P, B[*k*]FA, DB[*a,h*]A, and DB-[*a,c*]A were lower than the control level (0.6-, 0.7-, 0.7-, and 0.5-fold, respectively) (Figure 3C).

**Dose-Dependent Induction of mRNA of Metabolic Enzymes after Exposure to PAHs and Oxy-PAHs for 24 h.** The concentration-dependent induction of P450s, NQO1, and GSTM1 mRNA exposed for 24 h to B[*a*]P, B[*k*]FA, DB[*a,h*]A, IdP, NCQ, and B[*b*]FO was also examined (Figure 4). The $EC_{25}$ for the TCDD-dependent induction of P4501A1 mRNA in HepG2 cells was 68 pM (Figure 4A and Table 1). B[*a*]P was approximately 2000-fold less potent than TCDD. Also, in this experiment, PAHs such as B[*k*]FA and DB[*a,h*]A induced P4501A1 mRNA transcription much more strongly than B[*a*]P (100- and 6.7-fold IEF, respectively). Oxy-PAHs, NCQ, and B[*b*]FO induced P4501A1 mRNA transcription less strongly than B[*a*]P; nevertheless, these activities are considered to be high (0.66- and 0.58-fold IEF, respectively). Dose–response curves of P4501A2 mRNA inductions for the six compunds were quite similar to P4501A1, respectively (Figure 4B).

The order of the strength for NQO1 mRNA induction judged from the dose–response curves was as follows, B[*k*]FA, DB-[*a,h*]A, IdP > B[*a*]P, NCQ > B[*b*]FO, and slight NQO1 mRNA induction by 1.6 nM TCDD seemed to be observed (Figure 4C). GSTM1 mRNA induction was slightly decreased by concentration over 500 nM for B[*a*]P and B[*k*]FA and over 5 $\mu$M for DB[*a,h*]A and B[*b*]FO (Figure 4D).

**Time-Dependent Induction for mRNA of Metabolic Enzymes after Exposure by 5 $\mu$M PAHs and Oxy-PAHs.** Time–course induction levels of P4501A1, AKR1C1, NQO1, and GSTM1 mRNA by six representative 5 $\mu$M PAHs and oxy-PAHs (B[*a*]P, B[*k*]FA, DB[*a,h*]A, IdP, NCQ, and B[*b*]FO) were also examined (Figure 5). The induction of P4501A1 mRNA increased rapidly after exposure for six all PAHs and oxy-PAHs (Figure 5A) and was especially remarkable and continued through 48 h for B[*k*]FA and DB[*a,h*]A. Induction levels were almost constant after 6 h for NCQ and B[*b*]FO.

The mRNA induction of AKR1C1 increased quickly from 6 to 24 h for all PAHs and oxy-PAHs. The increase in rate for mRNA induction of AKR1C1 was higher for oxy-PAHs, NCQ, and B[*b*]FO than for nonoxy-PAHs (Figure 5B). The observed tendency was that the induction of AKR1C1 mRNA for all of the compounds started to decrease after 24 h.

The mRNA induction of NQO1 increased slowly at first but rose quickly from 6 to 24 h for most PAHs and oxy-PAHs. The increase in rate for the mRNA induction of NQO1 was slightly higher for oxy-PAHs, NCQ, and B[*b*]FO than for nonoxy-PAHs (Figure 5C). The induction of NQO1 mRNA started to decrease from about 24 h after for B[*a*]P, NCQ, and B[*b*]FO and was constant from 24 to 72 h for B[*k*]FA, DB-[*a,h*]A, and IdP. The observed tendency for GSTM1 mRNA showed slight decreases in induction for all PAHs and oxy-PAHs until 12 h. This tendency continued until 48 h for B[*a*]P and B[*k*]FA; however, the induction levels started to increase again after 12 h and exceeded control levels for B[*b*]FO, NCQ, IdP, and DB[*a,h*]A (Figure 5D).

## Discussion

Some of the main target organs for carcinogenesis by PAHs include lung, skin, and mammary glands; for example, mammal hepatoma cells are often used for examining metabolic enzyme induction and DNA adduct formation by PAHs such as B[*a*]P because the liver induces various metabolic enzymes at relatively high levels. It has also been suggested that liver metabolism plays a role for detoxification of PAHs and oxy-PAHs in local carcinogenesis; therefore, liver cells are appropriate for examining the induction patterns of enzymes related to detoxification.

Several research groups have reported induction of P4501A1 by PAHs in HepG2 cells (*12, 30, 35–40*), and the order for the strength of the induction was as follows: B[*k*]FA > DB[*a,h*]A > IdP > B[*b*]FA > B[*a*]P > Chr, B[*a*]A. This was determined from data utilizing the luciferase assay after 16 h and the immunoblot assay after 24 h (*37, 39*). These patterns were similar to our RT-PCR results after 24 h (Figure 4A). In this study, the levels of induction of P4501A1 mRNA by all 5 $\mu$M-dosed PAHs and oxy-PAHs did not decrease even after HepG2 cells were continually exposed for 72 h (Figure 5A). The mRNA half-life of P4501A1 is short (2.4 h), while the half-lives of both P4501A2 and P4501B1 mRNA are more than 24 h (*41*). It was reported that more than 75% of approximately 2 $\mu$M B[*a*]P was metabolized for 24 h in HepG2 cells and the tendency of metabolism for B[*k*]FA was similar to B[*a*]P (*37, 42*). Penning et al. suggested that one of the oxygenated metabolites of B[*a*]P, *o*-quinone (BPQ), also contributed to P4501A1 induction in HepG2 cells exposed to B[*a*]P. Therefore, it is possible that some oxygenated metabolites of B[*k*]FA contrib-

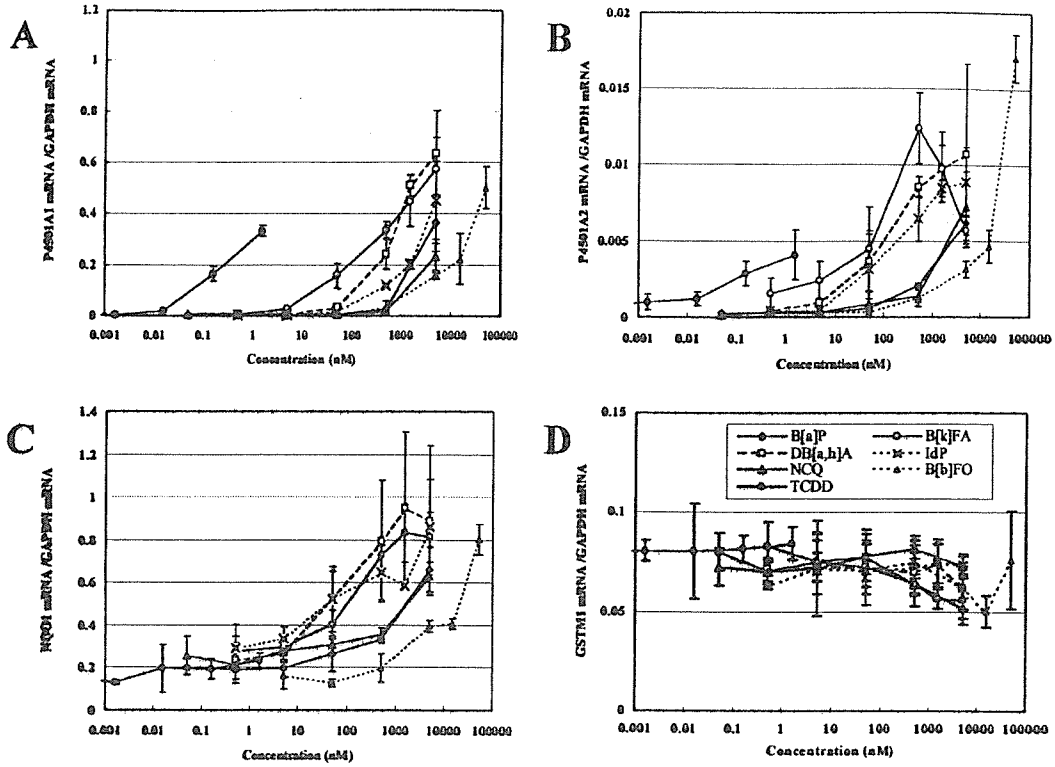


**Figure 4.** Dose-dependent induction for mRNA of metabolic enzymes measured by RT-PCR in HepG2 cells exposed to PAHs and oxy-PAHs for 24 h. (A) P4501A1 mRNA, (B) P4501A2 mRNA, (C) NQO1 mRNA, and (D) GSTM1 mRNA were measured.

**Table 1. P4501A1 mRNA Induction in HepG2 Cells (for 24 h) by PAHs, oxy-PAHs, and TCDD**

| compound | $EC_{TCDD25}$ (nM)[a] | IEF[b] |
|---|---|---|
| B[*a*]P | $1.3 \times 10^3$ | 1 |
| B[*k*]FA | 13 | 100 |
| DB[*a,h*]A | 200 | 6.7 |
| IdP | 350 | 3.8 |
| NCQ | $2.0 \times 10^3$ | 0.66 |
| B[*b*]FO | $2.3 \times 10^3$ | 0.58 |
| TCDD | 0.068 | $1.9 \times 10^4$ |

[a] Concentration equivalent with 25% of TCDD max (P4501A1 mRNA induction). [b] IEF relative to B[*a*]P (P4501A1 mRNA induction).

uted to the strong AhR-mediated induction of P4501A1 mRNA even after 72 h (*12*). It was shown that many DNA adducts caused by oxygenated metabolites such as hydroxyepoxides and bisdiols were formed when animals or culture cells were exposed to IdP and DB[*a,h*]A (*43, 44*). Indeed, high levels of formation of oxygenated metabolites may explain the strong P4501A1 mRNA induction for IdP and DB[*a,h*]A even after 72 h. In the case of oxy-PAHs NCQ and B[*b*]FO, continual P4501A1 mRNA induction, even after 72 h, may have been generated by oxygenated metabolites or ROS formation. The study for examining these possibilities is underway.

Penning et al. reported that the induction of AKR1C1 mostly occurred in four human isoforms of AKRs (AKR1C1–AKR1C4) when HepG2 cells and human colon carcinoma (HT29) cells were exposed to antioxidants such as $\beta$-NF and *tert*-butylhydroquinone and ROS such as $H_2O_2$ (*13*). They reported also that *trans*-dihydrodiols of some PAHs (naphthalene, phenanthrene, B[*a*]A, Chr, B[*a*]P, etc.) were converted to PAH catechols by several AKRs (*21*). In our study, the mRNA induction levels of AKR1C1 were significantly high at the exposure to 5 $\mu$M oxy-PAHs such as NCQ, B[*a*]FO, B[*b*]FO, CPPO, and $\beta$-NF (Figure 3A). The rapid increase for the induction of AKR1C1 mRNA via activated AP-1 was observed for oxy-PAHs NCQ and B[*b*]FO (Figure 5B); therefore, it is possible that these compounds themselves are AP-1 active compounds and AKR1C1 inducers. P450s-inducing PAHs such as B[*a*]P, B[*k*]FA, and DB[*a,h*]A at 5 $\mu$M also induced AKR1C1 mRNA significantly for 24 h, and the start of AKR1C1 mRNA inductions for B[*a*]P, B[*k*]FA, and DB[*a,h*]A required more than 6 h. Therefore, it is suggested that some P4501A1-catalyzed electrophilic oxygenated metabolites of PAHs (Michael reaction acceptors) or ROS generated from these metabolites contributed to the induction of AKR1C1 mRNA (Figures 2, 3A, and 5B).

Cytosolic NQO1 is the enzyme that catalyzes two-electron reduction and detoxification of quinones, repressing one-electron reduction of quinones by microsomal NADPH-dependent cytochrome P450 reductase and mitochondrial NADH-dependent ubiquinone oxidoreductase (*9, 15–17, 21, 28, 29, 45*). Several PAH quinones were reduced via both one- and two-electron reductions (*21, 29*). In our study, the mRNA induction levels of NQO1 were high after PAH exposure for 24 h at 5 $\mu$M except for TPh and B[*ghi*]Pe and this pattern is similar to P4501A1 and 1A2. However, the point that oxy-PAHs such as BAQ, NCQ, B[*a*]FO, B[*b*]FO, and $\beta$-NF at 5 $\mu$M induced NQO1 mRNA at the same levels as these nonoxy-PAHs was different from the patterns of P4501A1 and 1A2 mRNA induction. The tendency for a rapid increase in NQO1 mRNA induction from 6 h for most PAHs and oxy-PAHs is similar to AKR1C1 and the slightly higher rate increase of NQO1 mRNA induction for oxy-PAHs, NCQ, and B[*b*]FO, more than for nonoxy-PAHs, is also similar to AKR1C1 (Figure 5C). That the induction of NQO1 mRNA did not decrease from 24 to 72 h for B[*k*]FA, DB[*a,h*]A, and IdP is similar to P4501A1. NQO1 is regulated by both XRE (AhR) and EpRE (AP-1), so the result of the induction of NQO1 mRNA is thought to be the mixed type of

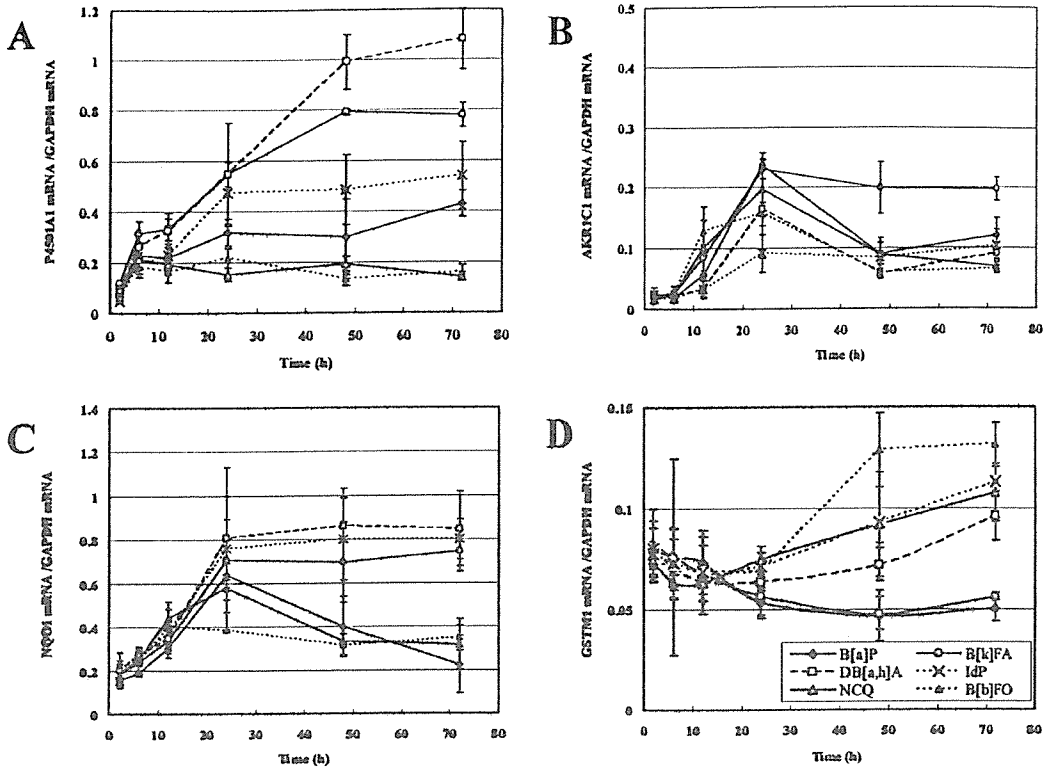


Figure 5. Time-dependent induction for mRNA of metabolic enzymes measured by RT-PCR in HepG2 cells exposed to 5 $\mu$M PAHs and oxy-PAHs. (A) P4501A1 mRNA, (B) AKR1C1 mRNA, (C) NQO1 mRNA, and (D) GSTM1 mRNA were measured.

P4501A1 mRNA and AKR1C1 mRNA based upon chemical dependency and time-dependent curves (Figures 2, 3, and 5). The contribution to NQO1 mRNA induction via EpRE (electrophiles or ROS) may be more than the contribution by AhR because the promoter of the human *NQO1* gene contains an imperfect XRE (*17*).

GSTAs, GSTMs, GSTPs, and GSTTs are included in human isoenzymes of GST (*17*, *46*, *47*). These GSTs catalyze GSH conjugation with ROS or B[*a*]P metabolites such as epoxides (BPDE, etc.) and quinones (BPQ, etc.) (*12*, *17*, *21*, *48*). In HepG2 cells exposed to a $Me_2SO$ control and some PAHs and oxy-PAHs, the mRNA levels of GSTA1 and GSTP1 were at least two magnitudes lower than GSTM1 in additional RT-PCR (data not shown); so, in this study, the GSTM1 isoform was measured in detail (*42*, *47*). The frequency of deficiency of the *GSTM1* gene is higher than other *GST* genes in humans (*14*, *17*), and the promoter of the *GSTM1* gene also contains both XRE and EpRE (*17*); however, in this study, mRNA induction was not dramatically increased by any PAH and oxy-PAH. Although the tendency for decrease in GSTM1 mRNA in the dose–response curves for several PAHs and oxy-PAHs and in the time–course curve for all PAHs and oxy-PAHs was observed and these decreases were much greater for B[*a*]P and B[*k*]FA, the mechanism of these phenomena was not clear (Figures 4D and 5D). It may be derived from a shortage of GSH during reactions with ROS or diolepoxides (*49*).

In conclusion, the pattern for induction of metabolic enzymes by three nonoxy-PAHs (B[*k*]FA, DB[*a*,*h*]A, and IdP) was similar to B[*a*]P. Considering this, mechanisms of metabolism by them are possibly similar to B[*a*]P. In the case of oxy-PAHs, the general mechanisms of induction of metabolic enzymes may be similar to that of quinone-yielding ROS (*21*, *45*). It will be necessary to examine the relationships between metabolite formation of PAHs and oxy-PAHs and DNA adduct formation and metabolic enzyme induction by them in detail. Additionally, it will be interesting to examine the patterns of metabolic enzyme induction and DNA adduct formation after compound exposure by using target organ cells in carcinogenesis studies in the future.

**Acknowledgment.** We thank Robert Kanaly, Department of Environmental Biosciences and International Graduate School of Arts and Sciences, Yokohama City University, Yokohama, Japan, for help in manuscript preparation. This work was supported in part from the Ministry of Health, Labour and Welfare and Grants-in-Aid for Scientific Research on Priority Areas (13027245, 16201012, and 18101003) from the Japanese Ministry of Education, Science, Sports and Culture.

## References

(1) Hannigan, M. P., Cass, G. R., Penman, B. W., Crespi, C. L., Lafleur, A. L., Busby, W. F., Jr., Thilly, W. G., and Simoneit, B. R. T. (1998) Bioassay-directed chemical analysis of Los Angeles airborne particulate matter using a human cell mutagenicity assay. *Environ. Sci. Technol. 32*, 3502–3514.

(2) Rogge, W. F., Hildemann, L. M., Mazurek, M. A., and Cass, G. R. (1993) Sources of fine organic aerosol. 2. Noncatalyst and catalyst-equipped automobiles and heavy-duty diesel trucks. *Environ. Sci. Technol. 27*, 636–651.

(3) Alsberg, T., Strandell, M., Westerholm, R., and Stenberg, U. (1985) Fractionation and chemical analysis of gasoline exhaust particulate extracts in connection with biological testing. *Environ. Int. 11*, 249–257.

(4) Fernandez, P., and Bayona, J. M. (1992) Use of off-line gel permeation chromatography-normal-phase liquid chromatography for the determination of polycyclic aromatic compounds in environmental samples and standard reference materials (air particulate matter and marine sediment). *J. Chromatogr. 625*, 141–149.

(5) IARC. (1983) Polynuclear aromatic compounds, Part 1, Chemical, environmental and experimental data. *IARC Monographs on the Evaluation of the Carcinogenic Risk of Chemicals to Humans*, Vol. *32*, IARC, Lyon, France.

(6) Monarca, S., Feretti, D., Zanardini, A., Moretti, M., Villarini, M., Spiegelhalder, B., Zerbini, I., Gelatti, U., and Lebbolo, E. (2001) Monitoring airborne genotoxicants in the rubber industry using genotoxicity tests and chemical analysis. *Mutat. Res. 490*, 159−169.
(7) Straif, K., Baan, R., Grosse, Y., Secretan, B., Ghissassi, F. E., and Cogliano, V. (2005) Carcinogenicity of polycyclic aromatic hydrocarbons. *Lancet Oncol. 6*, 931−932.
(8) Durant, J. L., Busby, W. F., Jr., Lafleur, A. L., Penman, B. W., and Crespi, C. L. (1996) Human cell mutagenicity of oxygenated, nitrated and unsubstituted polycyclic aromatic hydrocarbons associated with urban aerosols. *Mutat. Res. 371*, 123−157.
(9) Pelkonen, O., and Nebert, D. W. (1982) Metabolism of polycyclic aromatic hydrocarbons: Ethiologic role in carcinogenesis. *Pharmacol. Rev. 34*, 189−222.
(10) Møller, M., Hagen, I., and Ramdahl, T. (1985) Mutagenicity of polycyclic aromatic compounds (PAC) identified in source emissions and ambient air. *Mutat. Res. 157*, 149−156.
(11) Tada, K., Odashima, N., and Ishidate, M. (1966) On the screening experiment for the carcinogenesis of polycyclic quinones. *Kyoritsu Pharm. Univ. Environ. Doc.* 63−68.
(12) Burczynski, M. E., and Penning, T. M. (2000) Genotoxic polycyclic aromatic hydrocarbon *ortho*-quinones generated by aldo-keto reductases induce CYP1A1 via nuclear translocation of the aryl hydrocarbon receptor. *Cancer Res. 60*, 908−915.
(13) Burczynski, M. E., Lin, H.-S., and Penning, T. M. (1999) Isoform-specific induction of a human aldo-keto reductase by polycyclic aromatic hydrocarbons (PAHs), electrophiles, and oxidative stress: Implications for the alternative pathway of PAH activation catalyzed by human dihydrodiol dehydrogenase. *Cancer Res. 59*, 607−614.
(14) Sachse, C., Smith, G., Wilkie, M. J. V., Barrett, J. H., Waxman, R., Sullivan, F., Forman, D., Bishop, D. T., Wolf, C. R., and the Colorectal Cancer Study Group (2002) A pharmacogenetic study to investigate the role of dietary carcinogens in the etiology of colorectal cancer. *Carcinogenesis 23*, 1839−1849.
(15) Talalay, P. (1989) Mechanisms of induction of enzymes that protect against chemical carcinogenesis. *Adv. Enzyme Regul. 28*, 237−250.
(16) Prestera, T., Holtzclaw, W. D., Zhang, Y., and Talalay, P. (1993) Chemical and molecular regulation of enzymes that detoxify carcinogens. *Proc. Natl. Acad. Sci. U.S.A. 90*, 2965−2969.
(17) Hayes, J. D., and Pulford, D. J. (1995) The glutathione S-transferase supergene family: Regulation of GST* and the contribution of the isoenzymes to cancer chemoprotection and drug resistance. *Crit. Rev. Biochem. Mol. Biol. 30*, 445−600.
(18) Cavaieri, E. L., and Rogan, E. G. (1995) Central role of radical cations in metabolic activation of polycyclic aromatic hydrocarbons. *Xenobiotica 25*, 677−688.
(19) Melendez-Colon, V. J., Luch, A., Seidel, A., and Baird, W. M. (1999) Cancer initiation by polycyclic aromatic hydrocarbons results from formation of stable DNA adducts rather than apurinic sites. *Carcinogenesis 20*, 1885−1891.
(20) Park, J.-H., Troxel, A. B., Harvey, R. G., and Penning, T. M. (2006) Polycyclic aromatic hydrocarbon (PAH) *o*-quinones produced by the aldo-keto-reductases (AKRs) generate abasic sites, oxidized pyrimidines, and 8-oxo-dGuo via reactive oxygen species. *Chem. Res. Toxicol. 19*, 719−728.
(21) Bolton, J. L., Trush, M. A., Penning, T. M., Dryhurst, G., and Monks, T. J. (2000) Role of quinones in toxicology. *Chem. Res. Toxicol. 13*, 135−160.
(22) Kim, K. B., and Lee, B. M. (1997) Oxidative stress to DNA, protein, and antioxidant enzymes (superoxide dismutase and catalase) in rats treated with benzo(*a*)pyrene. *Cancer Lett. 113*, 205−212.
(23) Canova, S., Degan, P., Peters, L. D., Livingstone, D. R., Voltan, R., and Venier, P. (1998) Tissue dose, DNA adduct, oxidative DNA damage and CYP1A-immunopositive proteins in mussels exposed to waterborne benzo[*a*]pyrene. *Mutat. Res. 399*, 17−30.
(24) Leadon, S. A. (1987) Production of thymine glycols in DNA by radiation and chemical carcinogens as detected by a monoclonal antibody. *Br. J. Cancer 55* (Suppl.), 113−117.
(25) Vaghef, H., Wisén A.-C., and Hellman, B. (1996) Demonstration of benzo(a)pyrene-induced DNA damage in mice by alkaline single cell gel electrophoresis: Evidence for strand breaks in liver but not in lymphocytes and bone marrow. *Pharmacol. Toxicol. 78*, 37−48.
(26) Seike, K., Murata, M., Oikawa, S., Hiraku, Y., Hirakawa, K., Mimura, and Kawanishi, S. (2003) Oxidative DNA damage induced by benz-[*a*]anthracene metabolites via redox cycles of quinone and unique non-quinone. *Chem. Res. Toxicol. 16*, 1470−1476.
(27) Miller, K. P., Chen, Y.-H., Hastings, V. L., Bral, C. M., and Ramos, K. S. (2000) Profiles of antioxidant/electrophile response element (ARE/EpRE) nuclear protein binding and *c*-Ha-ras transactivation in vascular smooth muscle cells treated with oxidative metabolites of benzo[*a*]pyrene. *Biochem. Pharmacol. 60*, 1285−1296.
(28) Chesis, P. L., Levin, D. E., Smith, M. T., Ernster, L., and Ames, B. N. (1984) Mutagenicity of quinones: Pathways of metabolic activation and detoxification. *Proc. Natl. Acad. Sci. U.S.A. 81*, 1696−1700.
(29) Flowers-Geary, L., Harvey, R. G., and Penning, T. M. (1993) Cytotoxicity of polycyclic hydrocarbon *o*-quinones in rat and human hepatoma cells. *Chem. Res. Toxicol. 6*, 252−260.
(30) Staal, Y. C. M., van Herwijnen, M. H. M., van Schooten, F. J., and van Delft, J. H. M. (2006) Modulation of gene expression and DNA adduct formation in HepG2 cells by polycyclic aromatic hydrocarbons with different carcinogenic potencies. *Carcinogenesis 27*, 646−655.
(31) Streitwieser, A., Jr., and Brown, S. M. (1988) Convenient preparation of 11*H*-benzo[*a*]fluorenone and 11*H*-benzo[*b*]fluorenone. *J. Org. Chem. 53*, 904−906.
(32) Fieser, L. F., and Joshel, L. M. (1940) 9-Methyl-3,4-benzofluorene. *J. Am. Chem. Soc. 62*, 957−958.
(33) Spijker, N. M., van den Braken-van Leersum, A. M., Lugtenburg, J., and Cornelisse, J. (1990) A very convenient synthesis of cyclopenta-[*cd*]pyrene. *J. Org. Chem. 55*, 756−758.
(34) Clar, E., and Mackay, C. C. (1972) Circobiphenyl and the attempted synthesis of 1:14, 3:4, 7:8, 10:11-tetrabenzoperopyrene. *Tetrahedron 28*, 6041−6047.
(35) Adachi, J., Mori, Y., Matsui, S., and Matsuda, T. (2004) Comparison of gene expression patterns between 2,3,7,8-tetrachlorodibenzo-*p*-dioxin and a natural arylhaydrocarbon receptor ligand, indirubin. *Toxicol. Sci. 80*, 161−169.
(36) Iwanari, M., Nakajima, M., Kizu, R., Hayakawa, K., and Yokoi, T. (2002) Induction of CYP1A1, CYP1A2, and CYP1B1 mRNAs by nitropolycyclic aromatic hydrocarbons in various human tissue-derived cells: Chemical-, cytochrome P450 isoform-, and cell-specific differences. *Arch. Toxicol. 76*, 287−298.
(37) Vakhara, D. D., Liu, N., Pause, R., Fasco, M., Bessette, E., Zhang, Q.-Y., and Kaminsky, L. S. (2001) Polycyclic aromatic hydrocarbon/metal mixtures: Effect on PAH induction of CYP1A1 in human HepG2 cells. *Drug Metab. Dispos. 29*, 999−1006.
(38) Bessette, E., Fasco, M. J., Pentecost, T., and Kaminsky, L. S. (2005) Mechanisms of arsenite-mediated decreases in benzo[*k*]fluoranthene-induced human cytochrome P4501A1 Levels in HepG2 cells. *Drug Metab. Dispos. 33*, 312−320.
(39) Jones, J. M., and Anderson, J. W. (1999) Relative potencies of PAHs and PCBs based on the response of human cells. *Environ. Toxicol. Pharmacol. 7*, 19−26.
(40) Jones, J. M., Anderson, J. W., and Tukey, R. H. (2000) Using the metabolism of PAHs in a human cell line to characteraize environmental samples. *Environ. Toxicol. Pharmacol. 8*, 119−126.
(41) Lekas, P., Tin, K. L., Lee, C., and Prokipcak, R. D. (2000) The human cytochrome P450 1A1 mRNA in rapidly degraded in HepG2 cells. *Arch. Biochem. Biophys. 384*, 311−318.
(42) Plakunov, I., Smolarek, T. A., Fischer, D. L., Wiley, J. C., Jr., and Baird, W. M. (1987) Separation by ion-pair high-performance liquid chromatography of the glucuronide, sulfate and glutathione conjugates formed from benzo[a]pyrene in cell cultures from rodents, fish and humans. *Carcinogenesis 8*, 59−66.
(43) Nesnow, S., Ross, J. A., Mass, M. J., and Stoner, G. D. (1998) Mechanistic relationships between DNA adducts, oncogene mutations, and lung tumorigenesis in strain A mice. *Exp. Lung Res. 24*, 395−405.
(44) Rice, J. E., Coleman, D. T., Hosted, T. J., Jr., LaVoie, E. J., and Wiley, J. C., Jr. (1985) Identification of mutagenic metabolites of indeno-[1,2,3-*cd*]pyrene formed *in vitro* with rat liver enzymes. *Cancer Res. 45*, 5421−5425.
(45) Monks, T. J., Hanzlik, R. P., Cohen, G. M., Ross, D., and Graham, D. G. (1992) Quinone chemistry and toxicity. *Toxicol. Appl. Pharmacol. 112*, 2−16.
(46) Rowe, J. D., Nieves, E., and Listowsky, I. (1997) Subunit diversity and tissue distribution of human glutathione S-transferase: Interpretations based on electrospray ionization-MS and peptide sequence-specific antisera. *Biochem. J. 325*, 481−486.
(47) Aninat, C., Piton, A., Glaise, D., Charpentier, T. L., Langouët, Morel, F., Guguen-Guillouzo, C., and Guillouzo, A. (2006) Expression of cytochromes P450, conjugating enzymes and nuclear receptors in human hepatoma HepaRG cells. *Drug Metab. Dispos. 34*, 75−83.
(48) Sundberg, K., Dreij, K., Seidel, A., and Jernström, B. (2002) Glutathione conjugation and DNA adduct formation of dibenzo[*a*,*l*]-pyrene and benzo[*a*]pyrene diol epoxides in V79 cells stably expressing different human glutathione transferases. *Chem. Res. Toxicol. 15*, 170−179.
(49) Zhao, W., and Ramos, K. S. (1998) Cytotoxic response profiles of cultured rat hepatocytes to selected aromatic hydrocarbons. *Toxicol. in Vitro 12*, 175−182.

TX060197U

Int. J. Dev. Biol. 51: 000-000 UNCORRECTED PROOF (2007)
doi: 10.1387/ijdb.062139ku

*Short Contribution*

# Proprotein convertases modulate budding and branching morphogenesis of rat ventral prostate

KATSUNORI UCHIDA[1,2], MASAHIRO KANAI[1], SHIGENORI YONEMURA[1], KENICHIRO ISHII[1], YOSHIFUMI HIROKAWA[2] and YOSHIKI SUGIMURA[1,*]

*[1]Nephro-Urologic Surgery and Andrology, Division of Reparative and Regenerative Medicine and [2]Pathologic Oncology, Division of Molecular and Experimental Medicine, Mie University Graduate School of Medicine, Mie, Japan*

**ABSTRACT The onset of prostate morphogenesis is involved in the interaction between mesenchyme and epithelium. Proprotein convertases (PCs) activate a variety of growth and differentiation factors including mesenchymal and epithelial factors, such as insulin-like growth factor (IGF) and transforming growth factor-β (TGF-β), which induce ductal budding and branching. In this study, we provide evidence that PCs play a critical role in prostatic budding from the urogenital sinus (UGS) and ductal branching morphogenesis of the neonatal rat ventral prostate. PCs were expressed only in the epithelial cells of neonatal rat prostate. PC activity in the ventral prostate was modulated by endogenous androgen. PC inhibition suppressed prostatic budding and branching. Taken together, our data indicates that androgen-induced PCs initiate the development of the prostate.**

KEY WORDS: *proprotein convertase, prostate, development, furin, PC1*

Proprotein convertases (PCs) have been known as processing proteases that convert a wide variety of precursor proteins to their mature active form. To date, eight PCs have been identified including furin, PC1/3, PC2, PC4, PACE4, PC5/6 (and its isoform PC5B), PC7/8 and SKI-1. All PCs except for SKI-1 cleave precursor proteins at basic residues within the consensus motif (K/R)-$(X)_n$-(K/R)Ø, when n=0, 2, 4 or 6 and X is usually not Cys. All PCs except for SKI-1 are responsible for processing of matrix metalloproteinases (MMPs), growth factors, membrane receptors and adhesion molecules (Khatib *et al.*, 2004). Therefore, these processing enzymes are suggested to have a fundamental role in embryogenesis, development and disease via the activation of their substrates (Thomas 2002).

The prostate is a male sex accessory gland and develops from the embryonic urogenital sinus (UGS). Prostatic buds emerge from urogenital sinus epithelium (UGE) and extend into urogenital sinus mesenchyme (UGM) where they undergo ductal branching morphogenesis under androgenic stimulation of interactions between mesenchymal and epithelial cells (Sugimura *et al.*, 1986). In the developing prostate, both growth and differentiation factors are derived from mesenchyme via androgenic stimulation which induce prostatic epithelial growth (Hayward *et al.*, 2000). As candidates of these factors, insulin-like growth factor (IGF-1), hepatocyte growth factor (HGF), transforming growth factor-β (TGF-β), bone morphogenetic protein-4 (BMP-4) and prostate differentiation factor (PDF) were reported previously (Hayward *et al.*, 2000, Lamm *et al.*, 2001, Paralkar *et al.*, 1998). Many growth and differentiation factors are first synthesized as larger biologically inactive precursors, which are proteolytically activated by PCs. Previously we reported that the inhibition of PC activity resulted in the loss of the luminal cell phenotype and induction of the basal cell phenotype in LNCaP (Uchida *et al.*, 2003). Our results suggest that PCs activity may be involved in the regulation of prostate epithelial cell differentiation. The role of PCs in the development of the prostate remains largely unknown. Therefore, we hypothesized that PCs regulate budding and branching morphogenesis of the prostate epithelium via activation of growth and differentiation factors.

In this study, we investigated the distribution of PCs and the effect of the PCs inhibitor, decanoyl-Arg-Val-Lys-Arg-chloromethylketone (CMK) on prostatic bud formation from the UGS and the development of rat ventral prostate.

## Results and Discussion

### *PC expression in the UGS and neonatal rat prostate*

All PCs except for PC4, which is confined to the testis and ovary, are expressed widely in a variety of tissues and cells (Hatsuzawa *et al.*, 1990). However, the expression, localization

*Abbreviations used in this paper:* CMK, decanoyl-Arg-Val-Lys-Arg-chloromethylketone; IGF, insulin-like growth factor; PC, proprotein convertase; TGF, transforming growth factor; UGS urogenital sinus; VP, ventral prostate.

***Address correspondence to:** Dr. Yoshiki Sugimura. Nephro-Urologic Surgery and Andrology, Division of Reparative and Regenerative Medicine, Mie University Graduate School of Medicine, 2-174 Edobashi, Tsu, Mie, 514-8507 Japan. Fax: +81-59-231-5203. e-mail: sugimura@clin.medic.mie-u.ac.jp

0214-6282/2007/$30.00

Printed in Spain
www.intjdevbiol.com

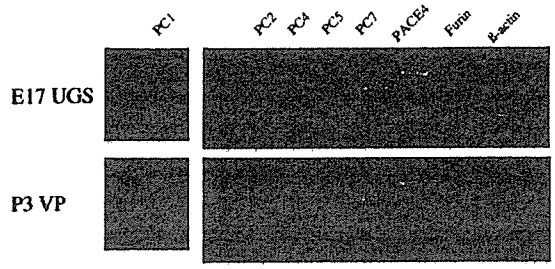


**Fig. 1. Proprotein convertase (PC) mRNA expression in E17 urogenital sinus (UGS) and P3 ventral prostate.** *Amplification products for PC1 and other PCs were separated by 2 % and 4 % agarose gel electrophoresis, respectively. PC2 mRNA was detected in the E17 UGS, not in the P3 ventral prostate*

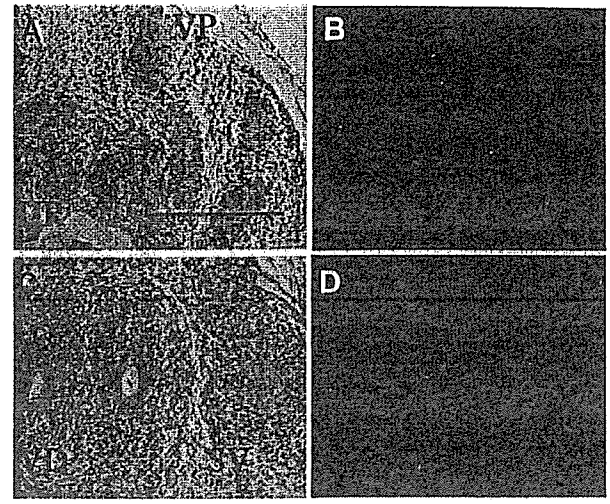


**Fig. 2. PC1 distribution in the developing prostate.** *Light micrographs of HE staining of P3 rat prostate* **(A,C)** *and immunostaining for PC1* **(B,D)**. *PC1-positive cells were detected in the epithelial cells of the VP (B), SV and VD (D). PC1 staining was not observed in the epithelial cells of the urethra and mesenchymal cells of the prostate. Abbreviations: SV, seminal vesicle; UR urethra; VD, vas deferens; VP, ventral prostate. Bar, 200 μm.*

and function of PCs in the prostate are still unknown. We first examined the gene expression and protein distribution of PCs in the developing prostate. Gene expressions of all PCs except for PC4 were detected in E17 UGS by RT-PCR. In contrast, PC2 and PC4 gene expression was not detected in P3 VP, whereas mRNAs of PC1, PC5, PC7, furin and PACE4 were observed (Fig. 1). Next we confirmed PCs expression and distribution by immunofluorescence staining. We examined the distribution of furin and PC1 in the developing prostate by immunofluorescence staining. At P3, cytoplasmic staining of PC1 was observed in the epithelial cells of the prostate, seminal vesicle and vas deferens. PC1 immunoreactivity was not observed in the mesenchymal cells of the prostate (Fig. 2). PC1 was also detected in endothelial cells and red blood cells. The distribution of furin-positive cells was similar to that of PC1-positive cells (data not shown). Furin and PC1 expressions were not observed in urethral mesenchyme and epithelium. At E17, furin and PC1 were detected in the epithelial cells of the vas deferens, but not epithelial cells of the UGS (data not shown). The discrepancy in PCs expression at UGS between RT-PCR and immunofluorescence staining could be due to the lower expression of PCs or the contamination of the vas deferens.

### *The modulation of PC activity in the neonatal ventral prostate*

Previous studies demonstrated that androgenic effects on epithelial growth, budding and ductal branching morphogenesis of the prostate were mediated by mesenchymal androgen receptors (Cunha *et al.*, 1980). Therefore, we hypothesized that the activity of epithelial PCs could be regulated by testosterone via epithelial-mesenchymal interaction. To investigate regulation of PCs activity by testosterone, E17 UGS and P1 VPs were cultured with or without testosterone. Comparable cultures were treated with CMK, the PC inhibitor. Results demonstrated that PCs activity was significantly increased by the addition of testosterone and PCs activity induced by testosterone was significantly inhibited by CMK at 50 μM in P1 VP (Fig. 3B), but not in E17 UGS (Fig. 3A).

Our results suggested that PC were expressed in the epithelium of the prostate during the period of budding and branching morphogenesis and that the activity of epithelial PCs was regulated by testosterone via epithelial-mesenchymal interaction. Our results also showed that testosterone treatment had minimal effect on P1 VP and did not affect PCs activity in UGS. These could be due to the lower activity of specific PC modulated by

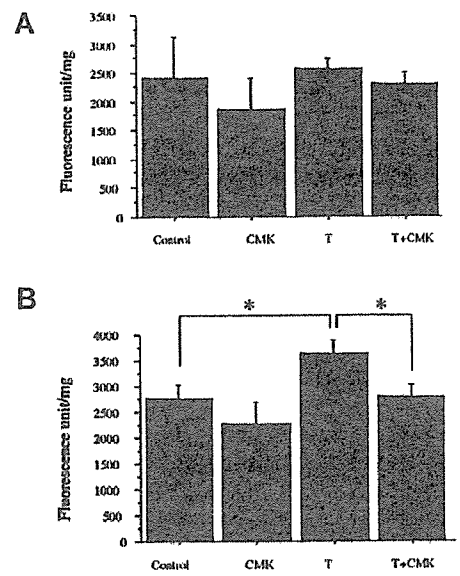


**Fig. 3. Proprotein convertase (PC) activity as measured by boc-RVRR-AMC processing. (A)** *The effect of 10 nM testosterone and 50 μM CMK on PC activity in the urogenital sinus. No significant differences were observed.* **(B)** *The effect of 10 nM testosterone and 50 μM CMK on PC activity of the rat P1 ventral prostate. PC activity was significantly increased by the addition of 10 nM testosterone. Testosterone-induced PC activity was significantly decreased by 50 μM CMK. *p < 0.05*

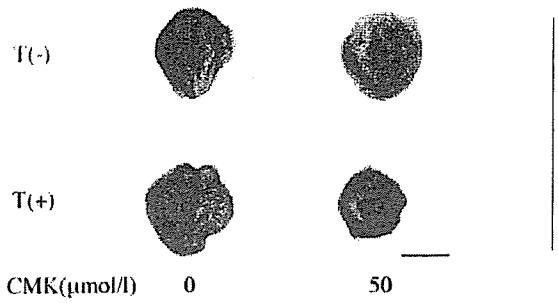


**Fig. 4. Effect of the proprotein convertase inhibitor, CMK, on prostatic bud formation**. *Representative images of rat urogenital sinus (UGS) cultured for 4 days in serum free medium without testosterone and CMK, with 10 nM testosterone alone, with both 50 μM CMK +10 nM testosterone and 50 μM CMK alone. Prostatic budding was observed by androgen stimulation. Androgen-stimulated budding was inhibited by treatment with 50 μM CMK. Bar, 1 mm.*

testosterone or the selectivity of boc-RVRR-AMC for specific PC, because wide variety of PCs was expressed in VP and UGS.

### *Effect of the proprotein convertase inhibitor, CMK, on prostatic bud formation and branching morphogenesis*

We next focused the effect of PCs on the prostatic budding and branching morphogenesis using *in vitro* organ culture system. Rat E17 UGS were cultured for 4 days and P1 VPs for 6 days. In the presence of testosterone at 10 nM, prostatic buds emerged from the UGE and elongated into the UGM. Testosterone-induced prostatic budding was inhibited by the addition of 50 μM CMK (Fig. 4). Neonatal VPs grew and underwent ductal brunching morphogenesis extensively with 10 nM testosterone. The addition of CMK inhibited the growth of neonatal prostate and significantly induced the reduction of the number of ductal tips with or without 10 nM testosterone in a dose- and a time-dependent manner (Fig 5A, B).

Histological and immunohistochemical analysis of cultured VPs was examined. Microscopically, the higher frequency of canalization was observed in the prostate treated with testosterone alone, not in the prostate with CMK (Fig. 6A). The diameter of ducts was significantly increased by the addition of CMK (Fig. 6B). In the prostate treated with testosterone alone, nuclear

TABLE 1

**PRIMERS USED FOR RT-PCR AMPLIFICATION**

| Gene | Primers | fragment size (bp) | Reference |
|---|---|---|---|
| PC1/3 | S: 5'-GCTACTAATCTCACTCAAAGC-3'<br>AS: 5'-CCTTCTCTTAATATGCCAAC-3' | 143 | Lee 1999 |
| PC2 | S: 5'-GCTAGACTTGAATGTGGC-3'<br>AS: 5'-GTTGCAGTCATCGTAGCT-3' | 525 | Rovere 1996 |
| PC4 | S: 5'-AGCCGCAACACATACACATC-3'<br>AS: 5'-GCCATCGCAGCATACAGTCA-3' | 680 | |
| PC5 | S: 5'-CTGCTGGTTTAAAGGTGAGCCA-3'<br>AS: 5'-TCACCAGCAGCTCTTTCTCC | 403 | Akamatsu 2000 |
| PC7 | S: 5'-GCCCAGGAAGAGACATCAAT-3'<br>AS: 5'-CATCTTGTCTCCTCCACTGA-3' | 640 | |
| PACE4 | S: 5'-CCCTCTGGAACCAAGTCTCAACTT-3'<br>AS: 5'-TGAAGCCAGCTTTACATCTGCTGC-3' | 1041 | Akamatsu 2000 |
| Furin | S: 5'-AATGGTGTCTGTGGTGTAGG-3'<br>AS: 5'-GTCAGCGTCCCATAGTTGTT-3' | 1050 | |

*S, sense; AS, antisense

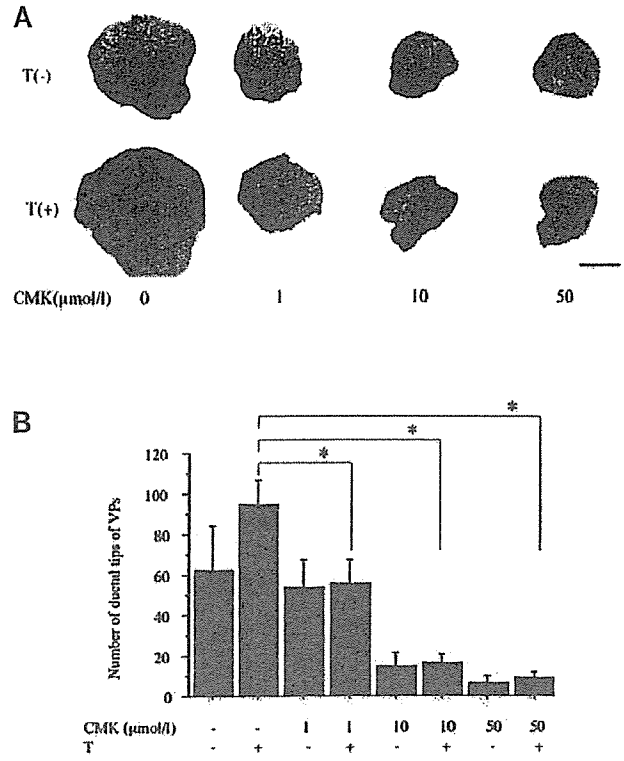


**Fig. 5. Effect of the proprotein convertase inhibitor, CMK, on branching morphogenesis. (A)** *Representative images of rat P1 ventral prostates cultured for 6 days in serum free medium with/without 10 nM testosterone, with various concentrations of CMK. Prostatic ductal growth and branching were observed by androgen stimulation. Androgen-stimulated growth was inhibited by treatment with CMK in a dose-dependent manner. Bar, 2 mm.* **(B)** *Quantification of branching with CMK treatment. Branching was significantly increased with testosterone and significantly inhibited by the addition of CMK in a dose-dependent manner. *p < 0.05*

staining of PCNA was more frequently observed in the ductal tip than in the base of the prostate by immunohistochemical staining. In contrast, PCNA expression was frequently observed in the tip and base of the prostate treated with testosterone + CMK (Fig. 6C).

Prostatic development is characterized by the bud formation, canalization and branching mediated via the epithelial-mesenchymal interaction under the balance of stimulatory and inhibitory factors. Among PCs substrates, IGF-1 and HGF are considered to be responsible for prostatic development as the stimulatory factors and BMP-4 is known as the inhibitory factor. TGF-β has the stimulatory effects on the periphery and inhibitory effects on the center of the prostate (Tomlinson *et al.*, 2004). In addition, previous study demonstrated that MMPs and integrins, which were considered as PCs substrates, also had the stimulatory effect on the branching of mammary gland and ureteric bud (Simian *et al.*, 2001, Pohl *et al.*, 2000, Zent *et al.*, 2001). PCs inhibition might cause an imbalance in the activation of stimulatory and inhibitory substrates. In fact, our macroscopic observa-

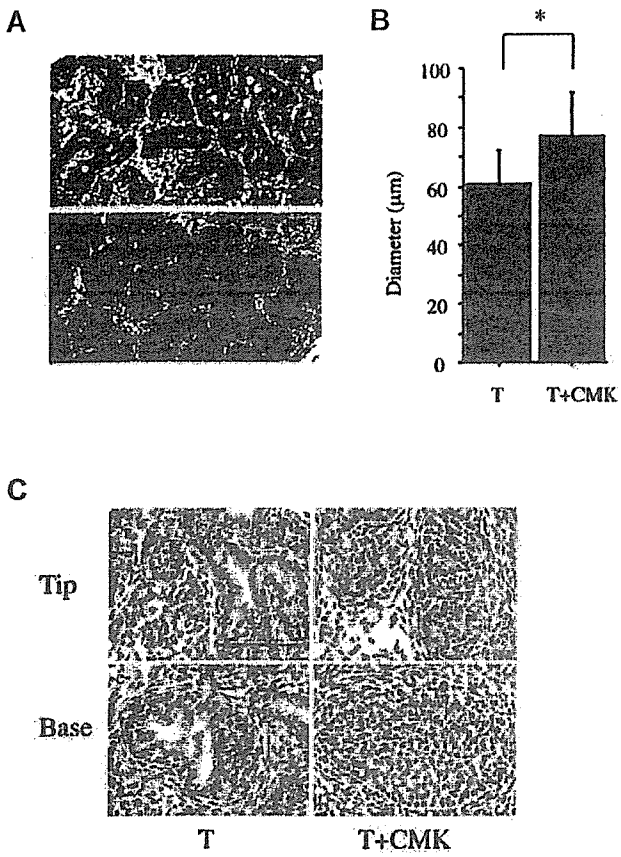


**Fig. 6. Effect of the proprotein convertase inhibitor, CMK, on branching morphogenesis – microscopic and immunohistochemical analysis. (A)** *Representative microscopic images (HE staining) of rat P1 ventral prostates cultured for 6 days in serum free medium with 10 nM testosterone, with/without 10 μM CMK. The higher frequency of canalization, the lower cell density of epithelium was observed in the prostate treated with testosterone without CMK (a), not in the prostate with CMK (b). Bar, 200 μm.* **(B)** *The diameter of ducts with testosterone, with/without CMK. The diameter was significantly increased by the addition of CMK. *p < 0.05.* **(C)** *Immunostaining for PCNA of the prostate treated with testosterone alone (a, c) and with testosterone and CMK (b, d). PCNA expression was observed in the ductal tip (a, b) and base (c, d). Bar, 200 μm.*

tion showed that PCs inhibitor reduced prostatic budding and branching, suggesting that BMP-4 activation might be accelerated by the inhibition of PCs. On the other hand, microscopic observation showed that PCs inhibitor induced the enlargement of the prostatic epithelial cord and the reduction of canalization. Thease results could be associated with the inactivation of morphogens, such as TGF-β and PDF, by the inhibition of PCs. In addition, PCNA expression indicated that PCs inhibitor initiated the epithelial proliferation in the base, which might represent the imbalance of the prostatic growth and be resulted in the enlargement of the prostatic epithelial cord. Our results indicate PCs are involved in the usual process of the prostatic development, including the budding, cord formation, canalization and branching. Therefore, the difference of the phenotypic expression in the prostate treated with or without PCs inhibitor would be important. The expression and localization of each PC, by which substrates are predominantly activated and responsible for the each steps of prostatic development, should be studied further.

In conclusion, our results suggest an important role of PCs in the prostatic morphogenesis. PCs modulated by androgen are expressed in neonatal VP and may be responsible for the processing of mesenchymal and epithelial factors, which initiate budding and branching of the prostate.

## Materials and Methods

### *Materials*

The animal use procedures were in accordance with the guide for the care and use of laboratory animals of Mie University Graduate School of Medicine. Sprague-Dawley (SD) rats were obtained from CLEA (Tokyo, Japan). Testosterone, insulin and transferrin were obtained from Sigma at MO. DMEM-Ham's F12 was purchased from Invitrogen (Carlsbad, CA), gentamycin from Wako (Osaka, Japan). N-t-butoxycarbonyl-Arg-Val-Arg-Arg-7-amino-4-methylcoumarine (Boc-RVRR-AMC) was obtained from Bachem (King of Prussia, PA) and decanoyl-Arg-Val-Lys-Arg-chloromethylketone (CMK) from Sigma (St. Louis, MO). Anti-furin and anti-PCNA antibodies were purchased from Santa Cruz (Santa Cruz, CA). Anti-PC1 antiserum was kindly gifted by Dr. Tanaka at Shizuoka University in Japan. FITC-labeled secondary antibody was purchased from MBL (Nagoya, Japan).

### *Tissue collection*

Rat UGS and VPs were obtained from SD rats. The day of detection of a vaginal plaque and the day of birth was designed E0 and P0, respectively. UGS from E17 rats and VPs from P0 and P3 neonatal rats were dissected and used for immunofluorescence staining, PC activity assay and *in vitro* organ culture.

### *RT-PCR Analysis*

Total RNA was prepared from E17 UGS and P3 VP using RNeasy (Qiagen, CA). cDNA was prepared using Superscript (Invitrogen, CA). The efficiency of each cDNA reaction was assayed by amplification of β-actin transcripts with primers for β-actin (R & D systems, MN). Primers used to amplify PCs gene were shown in Table1. The viability of the primer for PC4 was conformed using neonatal rat testis. The first strand cDNA was amplified with amplitaq gold (Applied biosystems, NJ). The PCR condition was as follows: 1 cycle at 95°C at for 5 min; 35 cycles at 95°C for 15 s, 53-57°C for 30 s, 72°C for 1 min 30 s. Amplification products (5 μl) were separated by 2-4% agarose gel electrophoresis.

### *Immunofluorescence staining*

Dissected E17 UGS and P3 prostate were fixed with 10% formaldehyde for 3 h on ice, processed into paraffin and then sectioned at 3 μm. Sections were deparaffinized with Histoclear. To enhance immunoreactivity for PCs, sections were oxidized before immunostaining with Gomori's oxidation mixture, as described previously (Kurabuchi and Tanaka, 1997). Rat pancreas was used as the positive control. Nonspecific binding was blocked with blocking buffer (DAKO, CA) for 1 hour at room temperature. Sections were sequentially incubated overnight at 4°C with following reagents: anti-furin antibody (1:50), anti-PC1 antiserum (1:500). The next day, sections were rinsed and incubated in a FITC-labeled secondary antibody and processed according to the manufacture's instructions.

### *Proprotein convertase activity assay*

E17 UGS and P1 VP were cultured with and without 10 nM testosterone and 50 μM CMK. After 24 h incubation, UGS and VP were washed with PBS and incubated with assay medium which consisted of the growth medium containing 0.25 % Triton X-100 to permeabilize cells and boc-RVRR-AMC (100 μM) as a fluorogenic substrate. Fluorescence was

measured at 360 nm excitation and 460 nm emission wavelengths after 4 h of substrate addition. Tissue weights of UGS and VPs were measured for normalization before the addition of assay medium. The data were normalized to tissue weights

**In vitro *organ culture***

UGS from E17 rats and VPs from P1 rats were grown in an organ culture system as previously described with modifications (Sugimura *et al.*, 1996). Briefly, dissected tissues were placed on Millicell membranes (Millipore, Bedford, MA) in 6-well plates (BD bioscience, Franklin Lakes, NJ) and cultured in DMEM-Ham's F12 without phenol red supplemented with insulin (10 μg/ml), transferrin (10 μg/ml) and gentamycin (50 μg/ml) at 5% $CO_2$. Testosterone (10 nM) and various concentrations of CMK were added and the medium was changed every day. Individual ductal tips were counted manually. Four to five VPs or UGSs were used for each group in one experiment. The experiment was repeated at least three times.

***Histological and immunohistochemical analysis of cultured VPs***

The prostates cultured with 10 nM testosterone with/without 10 μM CMK, were processed into paraffin and then sectioned at 3 μm. Sections were deparaffinized with Histoclear, used for Hematoxylin-Eosin (HE) staining and immunohistochemical staining. The diameter of the prostattic duct was measured under light microscope. Immunohistochemical staining was performed with Vectastain ABC kit (Vectastain Laboratories, CA). Briefly, sections were incubated overnight at 4°C with following reagents: anti-PCNA antibody (1:5000), The next day, sections were rinsed and incubated in a secondary antibody and processed.

***Statistical analysis***

Data are presented as the mean SD of four to five samples in each of two to six independent trials. Statistical analysis was performed using the Student *t* test. P value < 0.05 was considered significant.

*Acknowledgements*

*This work was supported by the Ministry of Education, Culture, Sports, Science and Technology of Japan (13671685, 14571495, 15390489), the Ministry of Health, Labor and Welfare of Japan (1700108-01) and Suzuki fundation of urology. We thank Dr. Tanaka for providing us anti-PC1 antiserum and Mrs. Hiroko Nishii for technical supports.*

## References

AKAMATSU, T., MATSUDA, Y., TSUMURA, K., TADA, J., PARVIN, M. N., WEI, W., KANAMORI, N. and HOSOI, K. (2000) Highly regulated expression of subtilisin-like proprotein convertase PACE4 (SPC4) during dentinogenesis. *Biochem. Biophys. Res. Commun.* 272, 410-415.

CUNHA, G. R., CHUNG, L. W., SHANNON, J. M. and REESE, B. A. (1980) Stromal-epithelial interactions in sex differentiation. *Biol. Reprod.* 22, 19-42.

TOMLINSON, D. C., FREESTONE, S. H., GRACE, O. C. and THOMSON, A. A. (2004) Differential effects of transforming growth factor-β1 on cellular proliferation in the developing prostate. *Endocrinology* 145, 4242-4300.

HATSUZAWA, K., HOSAKA, M., NAKAGAWA, T., NAGASE, T., SHODA, A., MURAKAMI, K. and NAKAYAMA, K. (1990) Structure and expression of mouse furin, a yeast Kex2-related protease. Lack of processing of coexpressed prorenin in GH4C1 cells. *J. Biol. Chem.* 265, 22075-22078.

HAYWARD, S. W. and CUNHA, G. R. (2000) The prostate: development and physiology, *Radiologic Clinics of North America* 38, 1-14.

KHATIB, A. M., SIEGFRIED, G., CHRETIEN, M., METRAKOS, M. and SEIDAH, N.G. (2002) Proprotein convertases in tumor progression and malignancy. *Am. J. Pathol.* 160,1921-1935.

KURABUCHI, S. and TANAKA S. (1997) Immunocytochemical localization of prohormone convertases PC1 and PC2 in the anuran pituitary gland: subcellular localization in corticotrope and melanotrope cells. *Cell Tissue Res.* 288, 485-496.

LAMM, M. L. G., PODLASEK, C. A. and BARNET, D. H. (2001) Mesenchymal factor bone morphogenetic protein 4 restrict ductal budding and branching morphogenesis in the developing prostate. *Dev. Biol.* 232, 301-314.

LEE, Y. C., DAMHOLT, A. B., BILLESTRUP, N,. KISBYE, T., GALANTE, P., MICHELSEN, B., KOFOD, H. and NIELSEN, J. H. (1999) Developmental expression of proprotein convertase 1/3 in the rat. *Mol. Cell Endocrinology* 155, 27-35.

PARALKAR, V. M., VAIL, A. L. and GRASSER, W. A. (1998) Cloning and characterization of a novel member of the transforming growth factor-β/bone morphogenetic protein family. *J. Biol. Chem.* 273,13760-13767.

POHL, M., SAKURAI, H., BUSH, K. T. and NIGAM, S. K. (2000) Matrix metalloproteinases and their inhibitors regulate in vitro ureteric bud branching morphogenesis. *Am. J. Physiology-Renal Physiology* 279, 891-900.

ROVERE, C., BARBERO, P. and KITABGI, P. (1996) Evidence that PC2 is the endogenous pro-neurotensis convertase in rMTC 6-23 cells and that PC1- and PC2-transfected PC12 cells differentially process pro-neurotensin. *J. Biol. Chem.* 271, 11368-11375.

SIMIAN, M., HIRAI, Y., NAVRE, M., WERB, Z., LOCHTER, A. and BISSELL, M. J. (2001) The interplay of matrix metalloproteinases, morphogens and growth factors is necessary for branching of mammary epithelial cells. *Development* 128, 3117-3131.

SUGIMURA, Y., CUNHA, G. R. and DONJACOUR, A. A. (1986) Morphogenesis of ductal networks in the mouse prostate. *Biol. Reprod.* 34, 961-71.

SUGIMURA, Y., FOSTER, B. A., HOM, Y. K., LIPSCHUTZ, J, H., RUBIN, J. S., FINCH, P. W., AARONSON, S. A., HAYASHI, N., KAWAMURA, J. and CUNHA, G. R. (1996) Keratinocyte growth factor(KGF) can replace testosterone in the ductal branching morphogenesis of the rat ventral prostate. *Int. J. Dev. Biol.* 40, 941-951.

THOMAS, G. (2002) Furin at the cutting edge: from protein traffic to embryogenesis and disease. *Nature Review Mol. Cell. Biol.* 10, 753-66.

UCHIDA, K., CHAUDHARY, L. R., SUGIMURA, Y., ADKISSON, H. D. and HRUSKA, K. A. (2003) Proprotein convertases regulate activity of prostate epithelial cell differentiation markers and are modulated in human prostate cancer cells. *J. Cell Biochem.* 88, 394-399.

ZENT, R., BUSH, K. T., POHL, M. L., QUARANTA, V., KOSHIKAWA, N., WANG, Z., KREIDBERG, J. A., SAKURAI, H., STUART, R. and NIGAM, S. K. (2001). Involvement of laminin binding integrins and laminin-5 in branching morphogenesis of the ureteric bud during kidney development. *Dev. Biol.* 238, 289-302.

*Received: 3rd January 2006*
*Reviewed by Referees: 12th April 2006*
*Modified by Authors and Accepted for Publication: 18h December 2006*
*Published Online: XX, 2007*

0163-4984/(Online)1559-0720/06/11300–0000 $30.00

# Correlation Between ZIP2 Messenger RNA Expression and Zinc Level in Rat Lateral Prostate

KAZUHIRO IGUCHI,[1] TAKASHI OTSUKA,[1] SHIGEYUKI USUI,[1] YOSHIKI SUGIMURA,[2] AND KAZUYUKI HIRANO*,[1]

[1]*Laboratory of Pharmaceutics, Gifu Pharmaceutical University, Mitahora-higashi, Gifu, Gifu 502-8585, Japan;* [2]*Department of Urology, Faculty of Medicine, Mie University, Edobashi, Tsu, Mie 514-8507, Japan*

Received September 13, 2005; Accepted October 25, 2005

## ABSTRACT

Zinc content in rat lateral prostate (LP) is higher compared with the other tissues, but the zinc retention system in the prostate remains unclear. In the present study, we examined the expression of ZRT, a IRT-like protein (ZIP) family transporter in rat prostate. The zinc level in rat LP was higher compared with the ventral (VP) and dorsal prostate (DP). The predicted ZIP2 mRNA was really expressed in LP at a high level. The expression was decreased in LP from castrated rats, associated with a decrease in zinc level, and these changes were prevented by testosterone replacement. Moreover, ZIP2 expression levels in LP positively correlated with the zinc levels. These findings strongly suggest that ZIP2 is involved in zinc homeostasis of rat prostate.

**Index Entries:** Zinc transporter; prostate; zinc; ZIP2; castration.

## INTRODUCTION

The prostate contains a higher concentration of zinc than any other tissues in the body *(1–3)*. Zinc is required for the activity of numerous metalloproteins *(4,5)*, for the optimal development and maintenance of the male reproductive system *(6,7)*, and for the antibacterial function in seminal plasma *(8)*. In prostate cancer, the zinc content is significantly lower than that in the surrounding normal prostate tissues *(9,10)* and the reduced zinc

*Author to whom all correspondence and reprint requests should be addressed.

content in the prostate tumor cells has been shown to lead to an increase in cell growth and invasion and a decrease in sensitivity to cytotoxic agents *(11–15)*. Zinc transporter (ZnT) 1 and ZnT4 expressions are decreased in patients with prostate cancer compared to those with benign prostatic hyperplasia although it is not clear whether the decrease in zinc level is the result of the change of the expression level *(16,17)*. Furthermore, the expressions of ZRT1, IRT1-like protein (ZIP) 1 and ZIP2 in prostate tumor tissues from African-American patients are lower compared with those from whites *(18)*. Thus, the functions of zinc and the differential expressions of zinc transporters in the prostate gland from the patients with prostatic diseases have been clarified gradually; however, the mechanism of zinc accumulation in the prostate gland remains unknown.

Many zinc transporters regulating zinc homeostasis have been identified in mammals. These include two families of zinc transporters: ZnT family (solute-linked carrier 30 (SLC30)) and ZIP family (solute-linked carrier 39 (SLC39)). ZnT and ZIP proteins appear to have opposite roles in cellular zinc homeostasis; that is, the ZnT proteins function in zinc efflux from cytoplasm or into intracellular vesicles, whereas the ZIP proteins function in zinc uptake into cells *(19,20)*. At present, four members of the ZnT family have been identified in the rat (ZnT1, ZnT2, ZnT3, and ZnT4), whereas ZIP family transporters have not been identified in the rat, but mRNA sequences of ZIP1 (accession no. XM_342286) and ZIP2 (XM_223975) predicted by automated computational analysis (NCBI annotation project) appear in GenBank. The predicted protein of ZIP1 (accession no. XP_342287.2) is 88% and 84% identical to the corresponding sequences from the mouse and human ZIP1, respectively, and that of ZIP2 (XP_223975.3) is also very similar to both mouse (95%) and human (76%) ZIP2 proteins.

The rat prostate gland is composed of at least three anatomically independent lobes, designated as ventral (VP), lateral (LP), and dorsal prostate (DP) *(21)*. The LP and DP are known to retain high levels of zinc in their lumen and epithelial cells *(22,23)*, and the level of zinc decreases in the LP following castration *(24–26)*. Thus, the zinc level in the prostate is affected by castration, but the mechanisms resulting in the change and the differential responsiveness among these lobes are obscure.

We have previously reported that ZnT2 is highly expressed in rat LP and DP *(27)*. The expression of ZnT2 mRNA is unaffected by castration, although the zinc level in the LP from castrated rats is lower than that in sham-operated rats, suggesting that ZnT2 is not involved in lowering the zinc content after castration *(27)*. As described earlier, ZnT family transporters are involved in the efflux of zinc, including from the cytoplasm out of the cell and into organellar compartments, whereas ZIP family transporters are involved in the influx of zinc into the cytosol, suggesting that a high concentration of zinc in the rat LP could be explained by the expression levels of ZIP family transporters, not but ZnTs. In this study, we attempted to determine the expression of ZIP transporters in the rat prostate by reverse transcriptase-polymerase chain reaction (RT-PCR) analysis.

## Materials and Methods

### Animal Protocol

Animal protocols were approved by the Animal Care and Use Committee of Gifu Pharmaceutical University. Male Sprague–Dawley rats were housed in an environmentally controlled room (25°C, 12-h light–dark cycle), and fed standard chow pellets and water ad libitum. Animals were divided into three groups: sham operation, castration, and testosterone replacement after castration. Castration was performed surgically under nembutal anesthetization via the scrotal route. After castration, animals from the testosterone-replacement group received a daily sc dose of 2 mg testosterone propionate (Sigma, St. Louis, MO) in corn oil. The treatment was started on the day following castration and continued for 14 d. All groups were killed at 14 d postcastration, and the VP, LP, and DP were collected. The tissues were rapidly removed after rats were killed and stored at –80°C until use.

### Semiquantitative Reverse Transcriptase–Polymerase Chain Reaction and Real-Time Quantitative RT-PCR

Total RNA was isolated using TRIzol reagent (Invitrogen, Carlsbad, CA, USA) according to the manufacturer's instructions. The extracted total RNA was dissolved in diethylpyrocarbonate (DEPC)-treated water and quantified by measuring the absorbance at 260 nm. Aliquots of 5 μg of total RNA were used to synthesize the first-strand cDNA with SuperScript III (Invitrogen) and subjected to PCR amplification with the following primers: ZIP1 sense, '-AAGCCTAGTGAGCTGCTTCG-3'; ZIP1 antisense, 5'-ACTGCCAGGATACCCTTGTG-3'; ZIP2 sense, 5'-CCCCTACGGA-GAACTTGTCA-3'; ZIP2 antisense, 5'-TACAGTAGCTGCCACGGTTG-3'; G3PDH sense, 5'-ATGACTCTACCCACGGCAAG-3'; G3PDH antisense, 5'-ACTGTGGTCATGAGCCCTTC-3'. The optimal PCR conditions were determined as the amount of amplification product in proportion to that of input RNA. PCR was performed under the following conditions: 28 cycles of 1 min at 94°C, 1 min at 60°C, and 1 min at 72°C for ZIP1; 30 cycles of 10 s at 95°C, 30 s at 64°C for ZIP2; 21 cycles of 1 min at 94°C, 1 min at 60°C, and 1 min at 72°C for glyceraldehyde-3-phosphate dehydrogenase (G3PDH). G3PDH served as an internal RNA control to allow comparison of RNA levels among different specimens. After PCR, the reaction products were resolved on 1.75% agarose gels and visualized with ethidium bromide.

Real-time monitoring of PCR reactions was performed using the iCycler iQ Real-Time PCR Detection System (Bio-Rad Laboratories, Hercules, CA, USA) with the iQ SYBR-Green Supermix reagents (Bio-Rad Laboratories). The following primers were used for PCR amplification reaction: ZIP2 sense, 5'-CTTCGGATTCCACAAGCATC-3'; ZIP2 antisense, 5'-TACAGTAGCT-GCCACGGTTG-3'; G3PDH sense, 5'-CTGCACCACCAACTGCTTAG-3';

G3PDH antisense, 5'-ACTGTGGTCATGAGCCCTTC-3'. The PCR was performed under the following conditions: 35 cycles of 10 s at 95°C, 30 s at 64°C for ZIP2; 35 cycles of 10 s at 95°C, 30 s at 65°C for G3PDH.

### Zinc Assay

The zinc assay was performed as described previously (27). Briefly, the samples were homogenized in 7 vol of Milli-Q water (Millipore Corp, Bedford, MA) and then digested in trichloroacetic acid/nitric acid (50/50) solution in a boiling water bath for 30 min. The digests were assayed for zinc by flame atomic absorption spectrometry (Shimadzu AA-6500).

### Protein Assay

Protein concentrations were determined by the Bradford assay (28) using bovine serum albumin (BSA) as a standard.

### Statistical Analysis

Statistical significance was assessed by one-way analysis (ANOVA) followed by Dunnett's test using PRISM4 software (Graphpad, San Diego, CA). A value of $p < 0.05$ was considered statistically significant.

## RESULTS

Zinc levels in the prostate from sham-operated, castrated, and testosterone-replaced rats are presented in Fig. 1. The zinc level in the LP of castrated rats was decreased as compared with that of sham-operated rats, and the decrease of zinc was prevented by testosterone replacement. No significant difference in zinc content of VP and DP was observed among the groups.

The expressions of ZIP transporters are shown in Fig. 2 (control). ZIP1 mRNA expression was detected in the VP, LP, and DP. ZIP2 mRNA was detectable in the LP, whereas weak and almost no signals were detected after 30 cycles of amplification in the DP and VP, respectively.

Because castration changed the zinc level in the rat LP, the expression levels of ZIP transporters in sham-operated, castrated, and castrated-testosterone-treated rats were investigated. As shown in Fig. 2, semiquantitative RT-PCR analysis showed that ZIP2 mRNA expression in LP was markedly decreased by castration and the decrease was prevented by testosterone replacement, which appeared to be correlated with the changes of zinc level in the LP. The mRNA expression of ZIP1 in the VP was increased 2.2±0.4-fold (as determined by Scion Image software) by castration, whereas no significant difference in the expression in the LP and DP was observed after castration. The increased ZIP1 expression by castration without change in zinc level indicates that ZIP1 is not involved

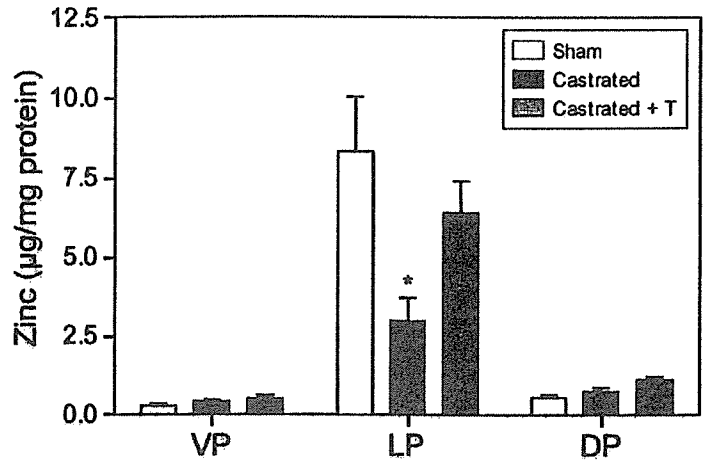


Fig. 1. Zinc levels in sham-operated, castrated, and castrated-testosterone (T)-treated rat prostate. The total zinc level of the prostate was determined as described in the Materials and Methods section. Values are expressed as the mean ± SEM of five animals. $^*p < 0.05$ vs sham-operated rats.

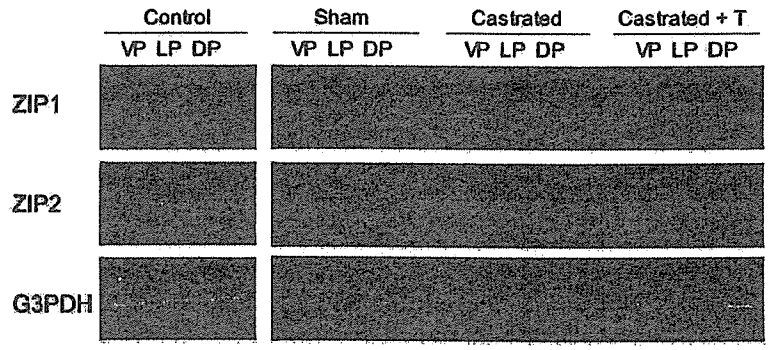


Fig. 2. RT-PCR analysis of ZIP1 and ZIP2 mRNA expression in rat prostates from control, sham-operated, castrated, and castrated-testosterone (T)-treated animals. Total RNA was purified from sham-operated, castrated, and castrated + T-treated rat prostate. The mRNA expression of ZIP1 and ZIP2 was examined by semiquantitative RT-PCR. The products were resolved on 1.75% agarose gels and visualized with ethidium bromide. Data shown are representative for five animals.

in zinc homeostasis in the VP. Therefore, we focused on ZIP2 in the following experiments.

Next, we performed real-time quantitative RT-PCR analysis to confirm the altered ZIP2 mRNA expression in the LP. Figure 3 shows that ZIP2 expression in the castrated rat LP was decreased to approx 22% of the sham-operated rat LP and recovered to approx 60% in the castrated-testos-

AU: "in the" ok?

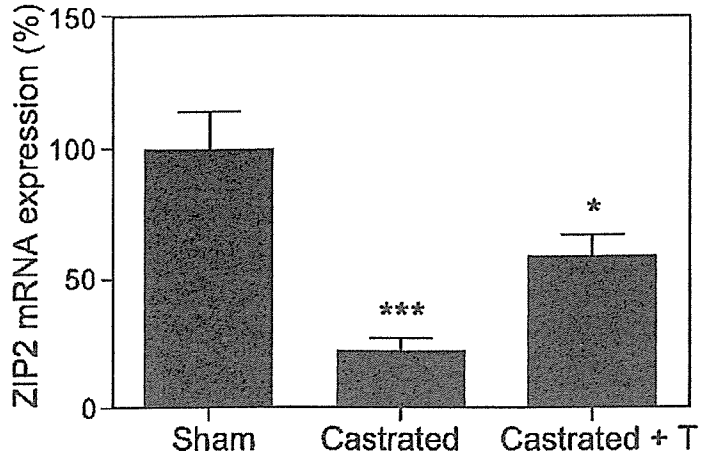


Fig. 3. Real-time quantitative RT-PCR analysis of ZIP2 mRNA in sham-operated, castrated, and castrated + T-treated rat LPs. The expression of the ZIP2 gene was normalized to G3PDH housekeeping gene expression. The level of ZIP2 mRNA expression in the sham-operated rat was set as 100%. Each column represents the mean ± SEM of five animals. $^{*}p < 0.05$, $^{***}p < 0.01$ vs sham-operated animals.

AU: 3 asteriks appear in the figure

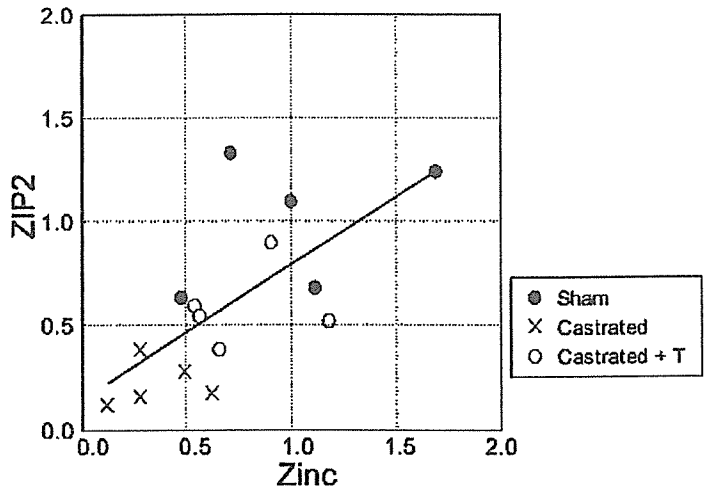


Fig. 4. Correlation between ZIP2 expression and zinc level in the LP. The zinc levels in the LP were plotted against the ZIP2 mRNA expression levels. The level of zinc content and ZIP2 mRNA expression in the sham-operated rat LP was set as 1.

terone-treated rat LP. Figure 4 shows the relationship between the zinc levels and the mRNA expressions of ZIP2 in the LP. There was a significant correlation between zinc levels and ZIP2 expressions ($r = 0.681$, $p < 0.01$).

## DISCUSSION

In this study, we found that predicted ZIP2 mRNA was really expressed in the LP, which contains a high level of zinc. The expression of ZIP2 in the LP decreased after castration and increased after testosterone replacement, and the decreased ZIP2 expression by castration in LP was accompanied by the reduction of zinc level. Moreover, there was a positive correlation between ZIP2 expression and zinc level in the LP. Although no studies on the zinc uptake function of rat ZIP2 protein have been reported, ZIP family transporters found in humans and the mouse function in zinc influx into cytosol from extracellular *(19,20)*, and in this study, the positive association was observed between ZIP2 expression and zinc level, strongly suggesting that rat ZIP2 could regulate zinc uptake in the LP. Additional study of zinc uptake function of rat ZIP2 will provide a better understanding of the role of the transporter in the rat prostate. In addition, it would be important to investigate the regulation of ZIP2 expression at the protein level. Because the rat ZIP2 protein has not been identified and an available anti-rat ZIP2 antibody is still not found, we could not examine the change of the expression of ZIP2 protein.

AU: "found in humans and the mouse" unclear, pls. check

The regulation of ZIP2 expression is mostly unknown. ZIP2 expression has been shown to be induced by the treatment of the intracellular zinc chelator TPEN [*N,N,N′,N′*-tetrakis(2-pyridylmethyl) ethylenediamine] in human monocytic THP-1 cells, indicating that ZIP2 expression could be regulated by zinc status *(29)*. In mouse intestine and visceral organs, the abundance of ZIP2 mRNA has not been affected by dietary zinc *(30)*. In this study, we found that the expression of ZIP2 in the LP decreased after castration and increased after testosterone replacement. Interestingly, the modification of ZIP2 gene expression was observed only in the LP, not in VP where androgen receptor is abundantly expressed compared to the LP *(31)*. It is unclear whether the change in ZIP2 expression is caused by either the altered androgen level or altered zinc level. However, because prolonged in vivo treatment of castration is known to induce the complex systemic changes such as atrophic effects and cell population changes *(26)*, it would not be possible from our in vivo data (castration for 2 wk) to determine whether the change in ZIP2 expression was caused by the specific effect of hormones.

We showed that ZIP1 mRNA was induced in the VP by castration. This is consistent with the finding that testosterone inhibited zinc accumulation in the VP *(26)*. On the other hand, our result seems to disagree with a previous study obtained in testosterone-treated LNCaP cells, showing that ZIP1 mRNA expression is stimulated by testosterone treatment *(32)*. The reason for the different result is not clear, but a possible explanation might be the differences in experimental conditions; that is, our result was obtained from in vivo experiments in the rat VP, whereas Costello et al.'s finding was from in vitro experiments using human LNCaP cells, which is likely more homologous to rodent LP than to the VP *(13)*. In addi-

tion, as discussed earlier, our in vivo regimens would not be sufficient to determine whether the altered ZIP1 expression was directly caused by hormonal effects.

AU: Costello et al.'s ok?

In conclusion, this is the first report of the finding of ZIP2 mRNA in the rat LP. In addition, the levels of zinc in the LP correlated significantly with the expressions of ZIP2 mRNA. The changes of zinc concentration in prostatic diseases have been well defined. The study of the relationship between ZIP2 expression and prostatic diseases might help in understanding prostatic diseases.

## REFERENCES


1. C. A. Mawson and M. I. Fischer, Zinc content of the genital organs of the rat, *Nature* **167,** 859 (1951).
2. C. A. Mawson and M. I. Fischer, The occurrence of zinc in the human prostate gland, *Can. J. Med. Sci.* **30,** 336–339 (1952).
3. C. A. Mawson and M. I. Fischer, Zinc and carbonic anhydrase in human semen, *Biochem. J.* **55,** 696–700 (1953).
4. A. S. Prasad, Zinc: an overview, *Nutrition* **11,** 93–99 (1995).
5. K. A. McCall, C. Huang, and C. A. Fierke, Function and mechanism of zinc metalloenzymes, *J. Nutr.* **130,** 1437S–1446S (2000).
6. A. E. Favier, The role of zinc in reproduction. Hormonal mechanisms, *Biol. Trace Element Res.* **32,** 363–382 (1992).
7. Y. Nishi, Zinc and growth, *J. Am. Coll. Nutr.* **15,** 340–344 (1996).
8. W. R. Fair, J. Couch, and N. Wehner, Prostatic antibacterial factor. Identity and significance, *Urology* **7,** 169–177 (1976).
9. F. Gyorkey, K. W. Min, J. A. Huff, and P. Gyorkey, Zinc and magnesium in human prostate gland: normal, hyperplastic, and neoplastic, *Cancer Res.* **27,** 1348–1353 (1967).
10. J. O. Ogunlewe and D. N. Osegbe, Zinc and cadmium concentrations in indigenous blacks with normal, hypertrophic, and malignant prostate, *Cancer* **63,** 1388–1392 (1989).
11. L. C. Costello, Y. Liu, R. B. Franklin, and M. C. Kennedy, Zinc inhibition of mitochondrial aconitase and its importance in citrate metabolism of prostate epithelial cells, *J. Biol. Chem.* **272,** 28,875–28,881 (1997).
12. K. Iguchi, M. Hamatake, R. Ishida, et al., Induction of necrosis by zinc in prostate carcinoma cells and identification of proteins increased in association with this induction, *Eur. J. Biochem.* **253,** 766–770 (1998).
13. J. Y. Liang, Y. Y. Liu, J. Zou, R. B. Franklin, L. C. Costello, and P. Feng, Inhibitory effect of zinc on human prostatic carcinoma cell growth, *Prostate* **40,** 200–207 (1999).
14. K. Ishii, S. Usui, Y. Sugimura, et al., Aminopeptidase N regulated by zinc in human prostate participates in tumor cell invasion, *Int. J. Cancer* **92,** 49–54 (2001).
15. K. Ishii, T. Otsuka, K. Iguchi, et al., Evidence that the prostate-specific antigen (PSA)/Zn2+ axis may play a role in human prostate cancer cell invasion, *Cancer Lett.* **207,** 79–87 (2004).
16. M. Hasumi, K. Suzuki, H. Matsui, H. Koike, K. Ito, and H. Yamanaka, Regulation of metallothionein and zinc transporter expression in human prostate cancer cells and tissues, *Cancer Lett.* **200,** 187–195 (2003).
17. S. M. Henshall, D. E. Afar, K. K. Rasiah, et al., Expression of the zinc transporter ZnT4 is decreased in the progression from early prostate disease to invasive prostate cancer, *Oncogene* **22,** 6005–6012 (2003).

18. I. Rishi, H. Baidouri, J. A. Abbasi, et al., Prostate cancer in African American men is associated with downregulation of zinc transporters, *Appl. Immunohistochem. Mol. Morphol.* **11,** 253–260 (2003).
19. M. L. Guerinot, The ZIP family of metal transporters, *Biochim. Biophys. Acta* **1465,** 190–198 (2000).
20. J. P. Liuzzi and R. J. Cousins, Mammalian zinc transporters, *Annu. Rev. Nutr.* **24,** 151–172 (2004).
21. N. Hayashi, Y. Sugimura, J. Kawamura, A. A. Donjacour, and G. R. Cunha, Morphological and functional heterogeneity in the rat prostatic gland, *Biol. Reprod.* **45,** 308–321 (1991).
22. J. A. Chandler, B. G. Timms, and M. S. Morton, Subcellular distribution of zinc in rat prostate studied by x-ray microanalysis: I. Normal prostate, *Histochem. J.* **9,** 103–120 (1977).
23. M. B. Sorensen, M. Stoltenberg, S. Juhl, G. Danscher, and E. Ernst, Ultrastructural localization of zinc ions in the rat prostate: an autometallographic study, *Prostate* **31,** 125–130 (1997).
24. B. G. Timms and J. A. Chandler, Effects of androgens on the ultrastructure and subcellular zinc distribution in the prostatic epithelium of castrated rats, *Prostate* **4,** 57–72 (1983).
25. A. Yamashita, N. Hayashi, Y. Sugimura, G. R. Cunha, and J. Kawamura, Influence of diethylstilbestrol, Leuprolelin (a luteinizing hormone-releasing hormone analog), Finasteride (a 5a-reductase inhibitor), and castration on the lobar subdivisions of the rat prostate, *Prostate* **29,** 1–14 (1996).
26. Y. Liu, R. B. Franklin, and L. C. Costello, Prolactin and testosterone regulation of mitochondrial zinc in prostate epithelial cells, *Prostate* **30,** 26–32 (1997).
27. K. Iguchi, S. Usui, T. Inoue, Y. Sugimura, M. Tatematsu, and K. Hirano, High-level expression of zinc transporter-2 in the rat lateral and dorsal prostate, *J. Androl.* **23,** 819–824 (2002).
28. M. M. Bradford, A rapid and sensitive method for the quantitation of microgram quantities of protein utilizing the principle of protein-dye binding, *Anal. Biochem.* **72,** 248–254 (1976).
29. J. Cao, J. A. Bobo, J. P. Liuzzi, and R. J. Cousins, Effects of intracellular zinc depletion on metallothionein and ZIP2 transporter expression and apoptosis, *J. Leukocyte Biol.* **70,** 559–566 (2001).
30. J. Dufner-Beattie, S. J. Langmade, F. Wang, D. Eide, and G. K. Andrews, Structure, function, and regulation of a subfamily of mouse zinc transporter genes, *J. Biol. Chem.* **278,** 50,142–50,150 (2003).
31. G. S. Prins, Differential regulation of androgen receptors in the separate rat prostate lobes: androgen independent expression in the lateral lobe, *J. Steroid Biochem.* **33,** 319–326 (1989).
32. L. C. Costello, Y. Liu, J. Zou, and R. B. Franklin, Evidence for a zinc uptake transporter in human prostate cancer cells which is regulated by prolactin and testosterone, *J. Biol. Chem.* **274,** 17,499–17,504 (1999).

Available online at www.sciencedirect.com
SCIENCE DIRECT
Cancer Letters 231 (2006) 304–308
CANCER Letters
www.elsevier.com/locate/canlet

# Existence of no-observed effect levels for 2-amino-3,8-dimethylimidazo[4,5-*f*]quinoxaline on hepatic preneoplastic lesion development in BN rats

Min Wei[a], Taka-aki Hori[b], Toshio Ichihara[a], Hideki Wanibuchi[a], Keiichirou Morimura[a], Jin Seok Kang[a], Rawiwan Puatanachokchai[a], Shoji Fukushima[a,*]

[a]*Department of Pathology, Osaka City University Medical School, 1-4-3 Asahi-machi, Abeno-ku, Osaka 545-8585, Japan*
[b]*Taishou Hospital, 5-5-16 Sankenya-higashi, Taishou-ku, Osaka 551-0002, Japan*

Received 21 December 2004; accepted 10 February 2005

**Abstract**

There is increasing evidence that dose–response curve of genotoxic carcinogen is nonlinear and a practical threshold dose exists. However, little is known about differences in the dose–response relationship of genotoxic carcinogen among different strain rats. Herein, we showed that low doses of genotoxic carcinogen 2-amino-3,8-dimethylimidazo[4,5-*f*] quinoxaline (MeIQx) had no effects on induction of liver glutathione S-transferase placental form (GST-P)-positive foci in both BN and F344 rats, and therefore demonstrated the existence of no-observed effect level for hepatocarcinogenicity of this genotoxic carcinogen irrespective of strains. These findings further support our notion that a practical threshold dose for MeIQx hepatocarcinogenicity exists in rats.


*Keywords:* 2-Amino-3,8-dimethylimidazo[4,5-*f*]quinoxaline; Cancer risk assessment; Hepatocarcinogenesis; No-observed effect level; Strain differences

## 1. Introduction

Exposure to environmental carcinogens is one of significant causes of human cancers. Some of environmental carcinogens cannot be completely eliminated, therefore, it is very important to assess and manage the potential risks associated with human exposure to these agents. Dose–response assessment

*Abbreviations* 2-AFF; 2-acetylaminofluorene; DEN; diethylnitrosamine; GST-P; glutathione S-transferase placental form; MeIQx; 2-amino-3,8-dimethylimidazo[4,5-*f*] quinoxaline; NOEL; no-observed effect level.

* Corresponding author. Tel.: +81 6 6645 3735; fax: +81 6 6646 3093.
*E-mail address:* fukuchan@med.osaka-cu.ac.jp (S. Fukushima).

0304-3835/$ - see front matter © 2005 Elsevier Ireland Ltd. All rights reserved.
doi:10.1016/j.canlet.2005.02.029